

## Stereospecificity in Reactions of Allylstannanes with Aldehydes Explored by Electronic Structure Calculations

Mark A. Vincent, Ian H. Hillier,\* Richard J. Hall, and Eric J. Thomas

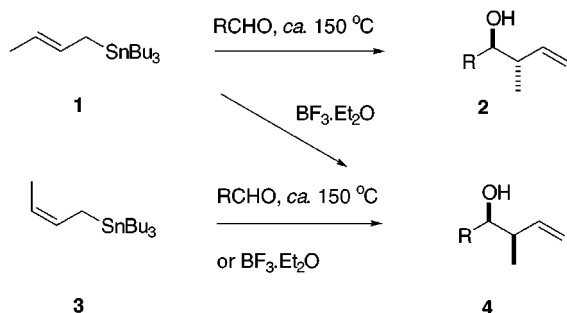
Department of Chemistry, University of Manchester, Manchester M13 9PL, U.K.

Received December 16, 1998

Electronic structure calculations at the 6-31G\*\*/B3LYP level have been used to identify stationary structures on the potential energy surfaces for reactions of 1-alkoxy- and 1-alkyl-alk-2-enylstannanes with aldehydes. The role of substituents at both the 1-position and at the tin center in determining the stereochemistry of the products and the size of the barriers to reaction have been explored. For alkyl substituents at the two positions, steric interactions lead to the *cis*-products being preferred, their preference increasing with the size of the substituents. Chloro-substitution at tin has both electronic and steric effects. The electron-deficient tin can form stronger bonding interactions, leading to barriers considerably lower than those for alkyl substitution. This is especially pronounced for 1-alkoxy substituents; only for the transition state leading to the *cis*-product is a six-coordinate tin arrangement found, with a correspondingly very low barrier.

### Introduction

Allylic organotin reagents have many uses in diastereoselective organic synthesis.<sup>1</sup> They react with aldehydes both on heating and at low temperatures in the presence of Lewis acids.<sup>2</sup> In many cases, these reactions show useful stereoselectivity. For example, the *anti*- and *syn*-alkenols **2** and **4** are obtained on heating mixtures of an aldehyde and the (*E*)- and (*Z*)-but-2-enylstannanes **1** and **3**, respectively, consistent with the participation of concerted processes involving chairlike, six-membered transition structures.<sup>3</sup> This selectivity contrasts with the



formation of the *syn*-isomer **4** as the major product from both the (*E*)- and (*Z*)-stannanes **1** and **3** at low temperature if the reaction is promoted by a Lewis acid, typically boron trifluoride diethyl etherate.<sup>4</sup> Activation of the aldehyde toward nucleophilic attack by coordination of the Lewis acid is believed to be involved in these reactions, although the geometry of the open-chain transition structure for the reaction of the coordinated aldehyde with the allylstannane is not fully established.<sup>5</sup>

(1) Thomas, E. J. In *Houben Weyl, Methods of Organic Chemistry*; Helmchen, G., Hoffmann, R. W., Mulzer, J., Schaumann, E., Eds.; Thieme: Stuttgart 1995; Vol. E21b, p 1508.

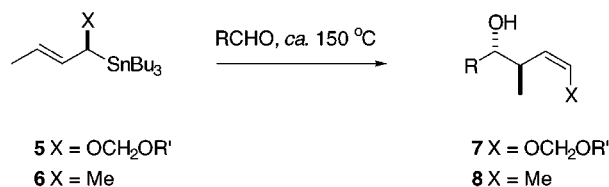
(2) Nishigaichi, Y.; Takuwa, A.; Naruta, Y.; Maruyama, K. *Tetrahedron* **1993**, *49*, 7395. Yamamoto, Y.; Shida, N. *Adv. Detailed React. Mech.* **1994**, *3*, 1.

(3) Servens, C.; Pereyre, M. *J. Organomet. Chem.* **1972**, *35*, C20.

(4) Yamamoto, Y.; Yatagai, H.; Ishihara, Y.; Maeda, N.; Maruyama, K. *Tetrahedron* **1984**, *40*, 2239. Keck, G. E.; Dougherty, S. M.; Savin, K. A. *J. Am. Chem. Soc.* **1995**, *117*, 6210.

Transmetalation of the allylstannane to generate a more reactive allyl organometallic reagent may also be involved in reactions of allylstannanes with aldehydes promoted by Lewis acids.<sup>6</sup>

Highly stereoselective reactions in favor of the *anti*-(*Z*)-isomers were discovered during a study of non-catalyzed reactions of 1-substituted but-2-enylstannanes with aldehydes.<sup>7</sup> For example, the *anti*-(*Z*)-enol ethers **7** were obtained with excellent stereoselectivity from the 1-alkoxybut-2-enylstannanes **5** and aldehydes at temperatures in the range 60–150 °C and similar stereoselectivity was observed with the 1-methylbut-2-enylstannanes **6**.<sup>8</sup> The stereoselectivities of these reactions are



consistent with the participation of six-membered, chairlike transition structures, (Figure 1), in which the substituents next to tin would appear to prefer axial rather than equatorial positions. This preference had been noted before in reactions with aldehydes of 1-substituted allyl-tin chlorides<sup>9</sup> and 1-chloro- and 1-methoxy-, but not 1-methyl-, allylboranes<sup>10</sup> and had been attributed to increased steric interaction between the 1-substituent

(5) Denmark, S. E.; Weber, E. J. *J. Am. Chem. Soc.* **1984**, *106*, 7970.

(6) Miyake, H.; Yamamura, K. *Chem. Lett.* **1993**, 1473. Keck, G. E.; Abbott, D. E.; Boden, E. P.; Enholm, E. J. *Tetrahedron Lett.* **1984**, *25*, 3927. Denmark, S. E.; Wilson, T.; Willson, T. M. *J. Am. Chem. Soc.* **1988**, *110*, 984. Denmark, S. E.; Weber, E. J.; Wilson, T. M.; Willson, T. M. *Tetrahedron* **1989**, *45*, 1053. Keck, G. E.; Andrus, M. B.; Castellino, S. *J. Am. Chem. Soc.* **1989**, *111*, 8136. Naruta, Y.; Nishigaichi, Y.; Maruyama, K. *Tetrahedron* **1989**, *45*, 1067. Boaretto, A.; Marton, D.; Tagliavini, G.; Ganis, P. *J. Organomet. Chem.* **1987**, *321*, 199.

(7) Pratt, A. J.; Thomas, E. J. *J. Chem. Soc., Perkin Trans. 1* **1989**, 1521. Jephcote, V. J.; Pratt, A. J.; Thomas, E. J. *J. Chem. Soc., Perkin Trans. 1* **1989**, 1529.

(8) Hull, C.; Mortlock, S. V.; Thomas, E. J. *Tetrahedron Lett.* **1987**, 5343. Hull, C.; Mortlock, S. V.; Thomas, E. J. *Tetrahedron* **1989**, *45*, 1007.

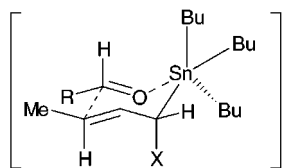


**Figure 1.** Suggested transition structure for reactions of stannanes **5** and **6** with aldehydes.

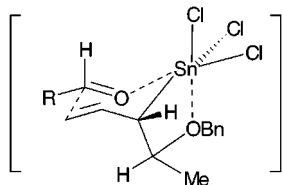
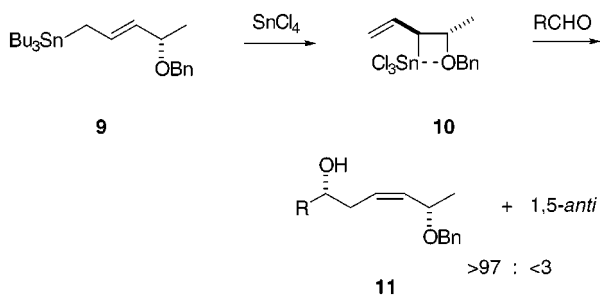


**Figure 2.** Suggested transition structure for reactions of allyltin trichloride **10** with aldehydes.

and the apical group on the tin or boron if the 1-substituent were to adopt the equatorial position.

The preference of a 1-substituent of an alk-2-enyltin reagent to adopt an axial rather than an equatorial position in a concerted reaction with an aldehyde has also been proposed for coordinated allyltin trihalides generated in situ from alkoxyalk-2-enylstannanes.<sup>11</sup> For example, treatment of the 4-benzyloxy-pent-2-enylstannane **9** with tin(IV) chloride generates an intermediate allyltin trichloride that reacts with aldehydes to give the 1,5-*syn* (*Z*)-products **11** with excellent overall stereoselectivity, 1,5-*syn*:1,5-*anti* = >97:<3.<sup>12</sup> It has been suggested that



this reaction involves the participation of the allyltin trichloride **10**, in which the vinyl and methyl substituents are *trans*-disposed about the four-membered ring formed by coordination of the alkoxy group to the electron-deficient tin, and that this intermediate reacts with the aldehyde via a six-membered chairlike transition structure, (Figure 2), in which the group next to tin is pseudoaxial.<sup>12</sup>

(9) Gambaro, A.; Boaretto, A.; Marton, D.; Tagliavini, G. *J. Organomet. Chem.* **1984**, *260*, 255. Miyake, H.; Yamamura, K. *Chem. Lett.* **1982**, 1369. Gambaro, A.; Ganis, P.; Marton, D.; Peruzzo, V.; Tagliavini, G. *J. Organomet. Chem.* **1982**, *231*, 307. Boaretto, A.; Marton, D.; Tagliavini, G.; Gambaro, A. *Inorg. Chim. Acta* **1983**, *77*, L196.

(10) Hoffmann, R. W.; Dresely, S.; Hildebrandt, B. *Chem. Ber.* **1988**, *121*, 2225. Hoffmann, R. W.; Landmann, B. *Angew. Chem., Int. Ed. Engl.* **1984**, *23*, 437. Hoffmann, R. W.; Dresely, S. *Angew. Chem., Int. Ed. Engl.* **1986**, *25*, 189. Hoffmann, R. W.; Dresely, S. *Chem. Ber.* **1989**, *122*, 903. Hoffmann, R. W.; Dresely, S. *Tetrahedron Lett.* **1987**, *28*, 5303. Andersen, M. W.; Hildebrandt, B.; Koster, G.; Hoffmann, R. W. *Chem. Ber.* **1989**, *122*, 1777. Hoffmann, R. W.; Dittrich, K.; Koster, G.; Sturmer, R. *Chem. Ber.* **1989**, *122*, 1783.

(11) Thomas, E. J. *J. Chem. Soc., Chem. Commun.* **1987**, 411. Thomas, E. J. *ChemTracts: Org. Chem.* **1994**, 207. Thomas, E. J. In *Stereocontrolled Organic Synthesis*; Trost, B. M., Ed.; Blackwell: London, 1994; p 235.

(12) McNeill, A. H.; Thomas, E. J. *Synthesis* **1994**, 322.

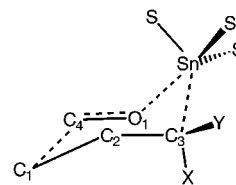


**Figure 3.** Atom labelling in transition structures.

We here report high level ab initio calculations that reveal more details of the transition structures proposed for reactions of 1-alkoxy- and 1-alkyl-alk-2-enylstannanes with aldehydes with modeling of transition structures in which the tin is trigonal bipyramidal, as in Figure 1, or octahedral, as in Figure 2.<sup>13</sup>

## Computational Methods

All calculations were carried out using Gaussian94<sup>14</sup> and a moderately large basis (6-31G\*\*) with electron correlation included using density functional theory (DFT) methods. We employed the B3LYP functional, Becke's three-parameter hybrid method.<sup>15</sup> We were concerned with a number of series of quite large molecular systems, the members of a series differing in the nature of particular substituents. For computational economy, not all individual stationary structures have been characterized because modest substitution (e.g., -H to -CH<sub>3</sub>) is not expected to change the topology of the minima and transition structures. However, representative structures were properly characterized by calculation of harmonic frequencies. Again, for reasons of computational economy, the calculations for those molecules having butyl groups were carried out using a hybrid quantum mechanical (QM)/molecular mechanical (MM) method.<sup>16</sup> Here, the terminal -C<sub>3</sub>H<sub>7</sub> part of the butyl group is represented by a generally accepted force field<sup>17</sup> that will properly describe its steric interactions with other groups. Geometry optimization of the QM region was then carried out, including its steric and electrostatic interactions with the MM butyl group.

## Computational Results

To understand the role of different substituents at tin (S) and at the 1-position, C<sub>3</sub> (X, Y) (Figure 3), in determining both the magnitude of the reaction barrier and the formation of *cis*(*Z*)- versus *trans*(*E*)-products, we have determined the stationary points on the potential energy surface of the reaction for a variety of these substituents.

The simplest model is for all three substituents to be hydrogen (X = Y = S = H) (I). Here, of course, there is a single product. The structures of the transition states for this and other systems are summarized in Table 1, with the corresponding barriers being given in Table 2. A chairlike transition structure was indeed found, in which

(13) Hobson, L. A.; Vincent, M. A.; Thomas, E. J.; Hillier, I. H. *J. Chem. Soc., Chem. Commun.* **1998**, 899.

(14) *Gaussian 94, Rev. D1*; Frisch, M. J.; Trucks, G. W.; Schlegel, H. B.; Gill, P. M. W.; Johnson, B. G.; Robb, M. A.; Cheeseman, J. R.; Keith, T. A.; Petersson, G. A.; Montgomery, J. A.; Raghavachari, K.; Al-Laham, M. A.; Zakrzewski, V. G.; Ortiz, J. V.; Foresman, J. B.; Cioslowski, J.; Stefanov, B. B.; Nanayakkara, A.; Challacombe, M.; Peng, C. Y.; Ayala, P. Y.; Chen, W.; Wong, M. W.; Andres, J. L.; Replogle, E. S.; Gomberts, R.; Martin, R. L.; Fox, D. J.; Binkley, J. S.; Defrees, D. J.; Baker, J.; Stewart, J. P.; Head-Gordon, M.; Gonzalez, C.; Pople, J. A. Gaussian, Inc.: Pittsburgh, PA, 1995.

(15) Becke, A. D. *J. Chem. Phys.* **1993**, *98*, 1372; **1993**, *98*, 5648.

(16) Harrison, M. J.; Burton, N. A.; Hillier, I. H. *J. Am. Chem. Soc.* **1997**, *119*, 12285.

(17) Pearlman, D. A.; Case, D. A.; Caldwell, J. C.; Seibel, G. L.; Singh, U. C.; Weiner, P.; Kollman, P. A. *AMBER 4.0*; University of California: San Francisco, 1992.

**Table 1. Transition Structures for Different Substituents (Å)<sup>a</sup>**

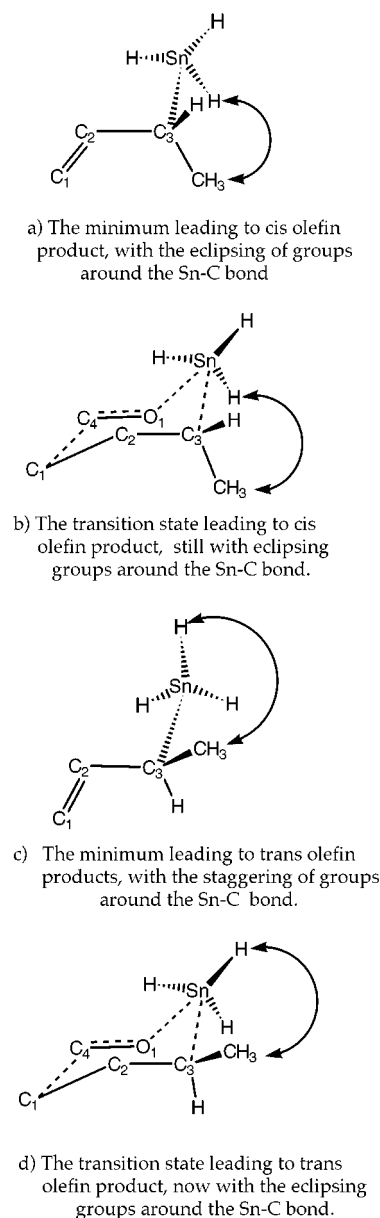
	X	Y	S	C <sub>1</sub> -C <sub>2</sub>	C <sub>2</sub> -C <sub>3</sub>	C <sub>3</sub> -Sn	Sn-O <sub>1</sub>	O <sub>1</sub> -C <sub>4</sub>	C <sub>4</sub> -C <sub>1</sub>
I	H	H	H	1.387	1.423	2.371	2.306	1.271	2.042
II	CH <sub>3</sub>	H	H	1.386	1.426	2.393	2.323	1.270	2.077
III	H	CH <sub>3</sub>	H	1.383	1.431	2.395	2.313	1.267	2.085
IV	H	H	CH <sub>3</sub>	1.385	1.421	2.390	2.363	1.267	2.071
V	CH <sub>3</sub>	H	CH <sub>3</sub>	1.385	1.424	2.414	2.375	1.266	2.108
VI	H	CH <sub>3</sub>	CH <sub>3</sub>	1.385	1.428	2.428	2.366	1.266	2.071
VII	CH <sub>3</sub>	H	Bu	1.382	1.424	2.440	2.407	1.261	2.156
VIII	H	CH <sub>3</sub>	Bu	1.382	1.427	2.464	2.406	1.261	2.061
IX	H	H	Cl	1.381	1.432	2.317	2.184	1.278	2.070
X	CH <sub>3</sub>	H	Cl	1.381	1.436	2.343	2.195	1.277	2.102
XI	H	CH <sub>3</sub>	Cl	1.381	1.439	2.363	2.187	1.277	2.068
XII	CH <sub>2</sub> OH	H	Cl	1.374	1.438	2.353	2.206	1.264	2.225
XIII	H	CH <sub>2</sub> OH	Cl	1.385	1.436	2.352	2.174	1.283	2.045
XIV	CH <sub>2</sub> OCH <sub>3</sub>	H	Cl	1.376	1.434	2.370	2.222	1.267	2.197
XV	H	CH <sub>2</sub> OCH <sub>3</sub>	Cl	1.387	1.432	2.372	2.184	1.284	2.043

<sup>a</sup> See Figure 3 for atom labeling.**Table 2. Calculated Barrier ( $\Delta E$ , kcal/mol) for Different Substituents**

	X	Y	S	$\Delta E$
I	H	H	H	9.3
II	CH <sub>3</sub>	H	H	8.0
III	H	CH <sub>3</sub>	H	9.2
IV	H	H	CH <sub>3</sub>	9.4
V	CH <sub>3</sub>	H	CH <sub>3</sub>	8.1
VI	H	CH <sub>3</sub>	CH <sub>3</sub>	10.8
VII	CH <sub>3</sub>	H	Bu	8.6
VIII	H	CH <sub>3</sub>	Bu	12.0
IX	H	H	Cl	3.8
X	CH <sub>3</sub>	H	Cl	3.5
XI	H	CH <sub>3</sub>	Cl	6.7
XII	CH <sub>2</sub> OH	H	Cl	1.5
XIII	H	CH <sub>2</sub> OH	Cl	8.9
XIV	CH <sub>2</sub> OCH <sub>3</sub>	H	Cl	1.9
XV	H	CH <sub>2</sub> OCH <sub>3</sub>	Cl	12.0

for the prototype system (I) ( $X = Y = S = H$ ), C<sub>1</sub>-C<sub>4</sub> is fairly long (2.042 Å), whereas the bonds to tin are in the range of 2.3–2.4 Å. The remaining bond lengths in the six-membered ring are between single and double bond values. This transition state corresponds to a barrier of 9.3 kcal mol<sup>-1</sup>.

When the allyl group has one methyl at C<sub>3</sub>, it is now possible in principle to obtain both cis- and trans-products. We have located the corresponding transition structures (II and III) (Table 1). These are both quite close to the structure for the unsubstituted system. The transition structure (III) that leads to the trans-product is higher in energy than the one for the cis-product (II) (9.2 compared to 8.0 kcal mol<sup>-1</sup> (Table 2)). However, by following the reaction path from the transition structure to reactants, we have found that different reactant conformations lead to the different isomeric products, the one giving the trans-product being the slightly more stable (by 0.5 kcal mol<sup>-1</sup>). Naturally, these two forms will be expected to rapidly interconvert at normal temperatures. These reactant structures are illustrated in Figure 4 and differ in the conformation about the Sn-C and C<sub>2</sub>-C<sub>3</sub> bonds, with the more stable staggered conformation leading to the trans-product. It is of interest that at our level of theory the eclipsed conformation that leads to the cis-product is indeed an energy minimum, confirmed by calculation of the harmonic frequencies, and not, as might be expected, a transition structure. We ascribe this effect to attractive interactions between the formaldehyde and allyl tin reactants which cause orientation around the Sn-C bond to be an eclipsed conformation. Examination of the (Sn)H-(CH<sub>3</sub>)H hydrogen-hydrogen non-

**Figure 4.** The different conformational minima and transition states of II and III.

bonded distances in the minima and transition structures reveals their role in determining the energetics of the isomeric structures. This distance is reduced from 3.268

Å in the reactant structure that leads to the trans-product to 2.491 Å in the corresponding transition structure. The corresponding values for the structures involved in the formation of the cis-product are 3.211 and 3.523 Å, respectively. The greater steric repulsion in the transition structure leading to the trans-product is evident. Thus, the conformation of the allyl group determines the relative stabilities of the two reactant structures that lead to cis- or trans-products, whereas the conformation about the Sn–C bond determines the relative barrier heights.

We now examine the effect on the barrier of substituents at the tin atom. Replacing all three hydrogen atoms by methyl groups ( $X = Y = H$ ;  $S = CH_3$ ) leads to a single product. The transition structure (IV) is very close to that for structure I, the corresponding barrier being essentially the same as that for I. However, further substitution when X or Y are methyl groups does lead to distinct transition structures that differ significantly in energy. Thus, for  $Y = CH_3$ ,  $X = H$ , leading to the trans-products, the barrier is 2.7 kcal mol<sup>-1</sup> greater than for  $Y = H$ ,  $X = CH_3$ , which yields the cis-product (Table 2). There is a correspondingly greater Sn–C<sub>3</sub> length (2.428 Å compared to 2.414 Å) in the former transition structure, which is presumably due to greater nonbonded H–H repulsion. Again there are different reactant conformations that lead to the two distinct transition states and hence products, with that yielding the trans-product being of lower energy, but only by 0.1 kcal mol<sup>-1</sup>. Thus, the different barrier heights that we have found are attributed to the nonbonded interactions between the (Sn)CH<sub>3</sub> and (C)CH<sub>3</sub> methyl groups. In the reactant conformation leading to the trans-product, the methyl group attached to the allyl fragment is staggered between two of the methyl groups attached to the tin, with closest approaches of 2.927 and 3.067 Å. In the reactant conformation leading to the cis-product, the methyl groups are now eclipsed, with a closest H–H nonbonded distance of 2.903 Å. The situation in the corresponding two transition structures is reversed, with the greater H–H nonbonded distance being for the structure that leads to the cis-product (3.025 Å compared to 2.345 Å), which is significantly lower in energy than the transition structure that yields the trans-product.

We see that there is an increasing differentiation in terms of energy between the transition structures that yield the two isomeric products as the size of the substituents at both Sn and C<sub>3</sub> increases. This trend continues when the substituents at the tin center become *n*-butyl (Table 2). The transition structure (VII) that gives the cis-product is again preferred over that which gives the trans-product (VIII), but here the energy difference is now 3.4 kcal mol<sup>-1</sup>, compared to a value of 2.7 kcal mol<sup>-1</sup> when the tin substituents were methyl (V and VI). The increased steric repulsion between the substituents at Sn and C<sub>3</sub> is clearly shown by the increased Sn–C<sub>3</sub> bond length in both transition structures (Table 1), which is especially evident in the higher energy structure (VIII).

A similar strategy was followed to study the role of different substituents on the potential energy surface for the corresponding reactions involving trichloro-allylstannanes. We first studied the reaction with hydrogens at C<sub>3</sub> ( $X = Y = H$ ;  $S = Cl$ ), which can yield only a single product (IX). In comparison with the reaction involving –SnH<sub>3</sub> ( $X = Y = Z = H$ ), we see (Table 1) that there are significant changes in the structure of the transition

state. The forming Sn–O bond is shorter (by 0.12 Å), as is the breaking Sn–C bond (by 0.05 Å). In addition, the barrier to the reaction is considerably reduced (from 9.3 to 3.8 kcal mol<sup>-1</sup>). The shorter Sn–O and Sn–C bonds in the transition state can be associated with a more energetically favorable structure leading to a lower barrier to reaction. We may ascribe these shortened bonds to the more favorable bonding interactions with the more positively charged tin atom, the increased positive charge being due to the three electronegative chlorine atoms. An increased interaction involving the tin atom is also found in the ground state, when a complex between the allyl tin and formaldehyde is found, having an oxygen–tin distance of 2.521 Å. In the corresponding reactants involving hydrogen and aliphatic groups bonded to the tin no such complex was found. Thus, for the trichloro species, formation of the transition state involves a quite modest reduction in the Sn–O length, from 2.521 to 2.184 Å, which also favors a low reaction barrier.

We next consider the effect of methyl substitution at C<sub>3</sub>, which can lead to both cis- and trans-products. As was found for the unchlorinated species (I–VIII), the major effect of methylation on the transition structures is to increase the length of the Sn–C<sub>3</sub> bond that is being broken. For the transition structure leading to the trans-product (XI), this length is greater than in the structure leading to the cis-product (X), as was found for aliphatic substitution at C<sub>3</sub>. Again, the barrier is lower for the less strained transition state (6.7 compared to 3.5 kcal mol<sup>-1</sup>) that leads to the cis-product. Such strain may be understood, at least semiquantitatively, in terms of the CH<sub>3</sub>–Cl interactions in the reactant complexes and in the corresponding transition structures. In the complexes leading to the cis- and trans-products (Figure 5a and 5c), such interaction is minimized as a result of the distance between the CH<sub>3</sub> group and the equatorial Cl that it eclipses (in Figure 5a) and (in Figure 5c) the fact that the CH<sub>3</sub> group is staggered with respect to an axial and equatorial Cl. In the transition structure leading to the cis-product (Figure 5b), the relative orientation of the CH<sub>3</sub> and Cl groups is preserved, whereas in the transition structure leading to the trans-product (Figure 5b), the CH<sub>3</sub> group now eclipses an axial Cl, leading to enhanced steric interaction and an increased barrier.

We now consider the case in which the substituent on the allyl group can itself interact with the tin center. The substituents we have chosen are CH<sub>2</sub>OH and CH<sub>2</sub>OCH<sub>3</sub>. In both cases, the oxygen atom of these groups bonds to the tin by lone pair donation. The reactant structures for these systems now involve octahedrally coordinated tin, with the oxygen atom of the substituted allyl group being 2.46–2.82 Å from the metal center. In the transition structures (Figure 6), the usual six-membered ring is found, but the 6-fold coordination about tin is not maintained in the structure that leads to the trans-product, with the Sn–O<sub>2</sub> distance being 3.547 and 3.464 Å for the CH<sub>2</sub>OH and CH<sub>2</sub>OCH<sub>3</sub> substituents, respectively. On the other hand, in the transition structure leading to cis-products, the Sn–O<sub>2</sub> bond is actually shorter in the activated complex than in the reactant structures. Thus, for CH<sub>2</sub>OH substitution, the Sn–O<sub>2</sub> length is reduced from 2.583 to 2.467 Å, and for CH<sub>2</sub>OCH<sub>3</sub>, the reduction is from 2.457 to 2.380 Å. It should also be noted that the forming C<sub>4</sub>–C<sub>1</sub> bond in these transition structures leading to cis-products is signifi-

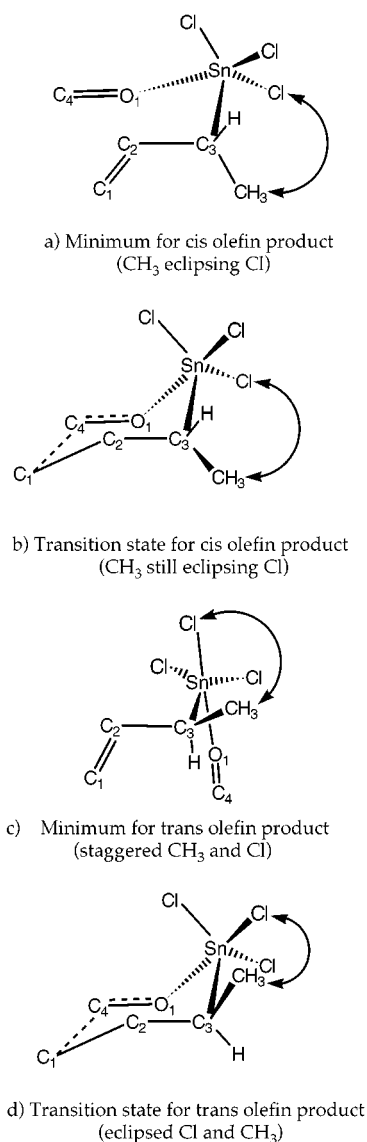


**Figure 5.** The minima and transition states of X and XI.

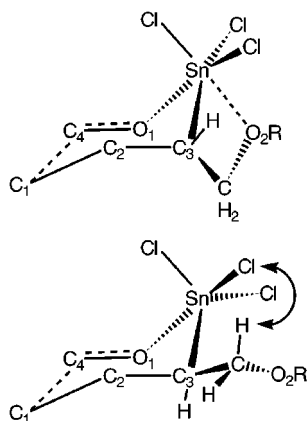


**Figure 6.** The cis and trans transition structures of the trichloro-tin and oxy-allyl ligand.

cantly longer than that found in other structures reported here, being 2.225 and 2.197 Å for CH<sub>2</sub>OH and CH<sub>2</sub>OCH<sub>3</sub>, respectively.

The unfavorable Sn–O<sub>2</sub> interactions in the higher energy transition structures (XIII and XV) may be ascribed to the steric interactions involving the bulky CH<sub>2</sub>OR group and the chlorine atoms, together with the configuration around C<sub>3</sub>, which does not allow a short Sn–O<sub>2</sub> distance. Because of this, we see here the greatest difference between the transition structures that yield the cis- and trans-products. This is reflected in the large difference in the corresponding barriers (2 compared to 9–12 kcal mol<sup>-1</sup>), which predicts a very facile reaction to form the cis-product.

## Conclusion

We first note that we have checked the accuracy of the DFT method, used here, by evaluating the barrier for reaction VI (Table 2) at the MP2 level, using the DFT stationary structures. A barrier of 12.4 kcal mol<sup>-1</sup> was obtained, compared to 10.8 kcal mol<sup>-1</sup> from the DFT calculation. We also note that our calculations are for 0 K.

The calculations described herein have resulted in a quantitative understanding of the interactions responsible for both the stereoselectivity and the relative ease of the reactions involving an important class of allylic organotin reagents. A far greater range of substituents at both the tin center and at the 1-position can be considered by accurate modeling methods than can be readily explored synthetically. The calculations show that the interactions between the substituents at these two positions are responsible for the observed stereospecificity. For alkyl substituents, the tin is five-coordinate. The preference for the cis-product increases as the degree of substitution and the bulk of the substituents increase, with the predicted barriers being in the range 8–12 kcal/mol. The effects of chloro groups at the tin atom are rather more pronounced. The electron-withdrawing effect of the halogens results in an electron-deficient tin atom that can form stronger interactions with its other neighbors, which in the absence of other steric interactions can result in transition state stabilization and quite low barriers, as well as greater discrimination between cis- and trans-products than was evident for alkyl substitution. This effect is especially evident for CH<sub>2</sub>OR substituents at the 1-position, where a six-coordinate tin arrangement is possible in the transition state that leads to the cis-product and results in a very low barrier (~2 kcal/mol). However, steric interactions prevent such a high tin coordination in the corresponding transition state leading to the trans-product.

**Acknowledgment.** We thank EPSRC for support of this research.

**Supporting Information Available:** Cartesian coordinates for the tin allyl species considered. This material is available free of charge via the Internet at <http://pubs.acs.org>.

JO9824551